Engineering Structures 244 (2021) 112741

Contents lists available at ScienceDirect

Engineering Structures

journal homepage: www.elsevier.com/locate/engstruct

An alternative experimental methodology to determine the diagonal cracking resistance of steel-reinforced concrete beams

Jesús M. Romera [a,*], Ignacio Marcos [a], Marta Skaf [b], Vanesa Ortega-López [b]

[a] Department of Mechanical Engineering, Faculty of Engineering of Bilbao, University of the Basque Country UPV/EHU, Rafael Moreno "Pitxitxi" 2, 48013 Bilbao, Spain
[b] Department of Civil Engineering, Higher Polytechnic School, University of Burgos, Calle Villadiego s/n, 09001 Burgos, Spain

ARTICLE INFO

Keywords:
Diagonal shear resistance
Steel-reinforced concrete
Extensometric gauges
Electric arc furnace slag aggregate

ABSTRACT

An alternative experimental method for predicting the diagonal shear cracking resistance of steel-reinforced concrete beams is developed in this paper. Conventional extensometric strain-gauge rosettes are placed on the lateral surfaces of a set of four beams. As diagonal cracking propagates through the beams, the load–strain curves flatten out at a plateau and the mechanical property under consideration may be determined. The method is applied to four beams cast from pumpable and self-compacting concrete mixes with cement types I and IV containing electric arc furnace slag aggregates. The feasibility of applying standard design code formulas to the concretes containing these aggregates may therefore be studied and compared with other recent research works. Accurate experimental results were obtained with this method without having to interrupt the test for subjective visual appraisals of the test specimen.

1. Introduction

Using the conservative formulas of standard design codes is a safeguard against failure mechanisms. However, if a non-conventional concrete type that is not specified in the design codes is used or non-static or temperature loading is applied, then the mechanical behavior requires further investigation. Currently, a new generation of green concretes based on the use of industrial by-products is under development in the framework of the circular economy. Several studies have been carried out, in order to assess their behavior and applicability to building [1–6]. However, research on their mechanical behavior at the structural or macro level is scarce [7–9]. A key property that must be checked during the Ultimate Limit State Design of Steel Reinforced Concrete (SRC) beams is resistance to shear failure or shear capacity. For instance, when the risk of earthquakes is high, it would be of interest to implement structural monitoring by means of non-destructive methods such as acoustic emissions [10].

The first sign of shear failure is a critical diagonal crack, the width of which increases until the applied load reaches the ultimate shear strength. The diagonal crack load is referred to as the load at which the first diagonal crack occurs. Determination of the onset of diagonal cracking in structural concrete elements is essential to analyze their behavior under shear loading. On the one hand, the diagonal crack plays a decisive role in the ultimate shear strength [11,12]. On the other hand, the diagonal shear crack load is necessary to determine the reserve shear strength factor. The reserve shear strength factor is defined as the ratio of the ultimate shear load to the diagonal shear cracking resistance [13]. When analyzing the reserve shear strength factor, the effects of concrete mixtures on shear resistance, such as aggregate interlock, must be taken into account. The safety margin of each material between the first diagonal crack and the ultimate shear failure is a key parameter. Although the pioneering study of Yang *et al.* [13] was on high-strength concrete deep beams without stirrups, the reserve shear strength parameter was computed later in other studies when analyzing the behavior of SRC beams with stirrups in the case of concrete with recycled aggregates [14] and self-compacting concrete (SCC) [15].

Diagonal cracking in SRC beams without stirrups has been extensively studied. It is mainly influenced by the shear span to effective depth ratio, a/d, the section height, h, and the concrete compression strength, f_c [16]. The influence of the shear-span-to-depth ratio on diagonal shear cracking resistance has been reported in various papers [17,18]. Sato and Kawakane [19] assessed the influence of early-age-shrinkage on the diagonal cracking of High-Strength SRC beams. In contrast to the strength analysis of the beams under flexural loading, the analysis in the case of shear loads is a complex problem. There is a lack of analytical solutions for the distribution of shear stress in cross-

* Corresponding author.
E-mail address: jesusmaria.romera@ehu.eus (J.M. Romera).

https://doi.org/10.1016/j.engstruct.2021.112741
Received 11 January 2021; Received in revised form 27 May 2021; Accepted 16 June 2021
Available online 24 June 2021
0141-0296/© 2021 The Authors. Published by Elsevier Ltd. This is an open access article under the CC BY license (http://creativecommons.org/licenses/by/4.0/).

Table 1
Hardened properties of the mixes.

Mixture	E^{*} (GPa)	Poisson's ratio (ν)	Compressive strength** (MPa)	Direct tensile strength*** (MPa)
IP	38.6	0.23	42–53-63–64-64	3.91
IVP	31.4	0.22	18–29-36–48-56	2.83
ISC	39.9	0.22	42–53-66–76-77	4.19
IVSC	33.8	0.21	19–31-37–55-62	3.69

* : after 90 days.
** : after 7–28-90–180-360 days in a moist room.
*** : after 180 days.

Table 2
Compressive strengths after 28 days (MPa).

	S1	S2	S3	Mean value
IP	49	54	56	53
IVP	24	30	33	29
ISC	50	53	55	53
IVSC	28	32	33	31

sections of composite materials [20]. It is therefore necessary to use some hypotheses, which simplify the problem and experimental correlations, as with the design code formulas. Various expressions for predicting the initiation of diagonal cracking can be found in ACI 318 [21] and Eurocode 2 [22]. It is worth underlining that the interest in the formulas of these codes is based on their simplicity and generality, hence their use in the design of real structures. However, their poor accuracy when applied to diagonal cracking resistance [23] can be improved with the formulations of some authors. Wu and Hang [24] presented a simple formula for predicting the initial diagonal cracking load in ultra-high-performance fiber-reinforced concretes. In the case of slender RC beams without stirrups, Keskin and Arslan [25] and Al-Zoubi [26] used an artificial neural network model and a shear-moment interaction model, respectively. Javidmehr *et al.* [27] proposed a simple and accurate formula with the following terms: shear span ratio, longitudinal reinforcement ratio and concrete strength.

Fig. 4. Left shear span of the IP beam.

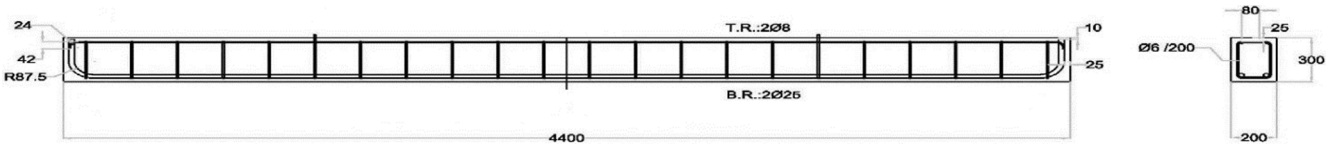

Fig. 1. Beam reinforcement details.

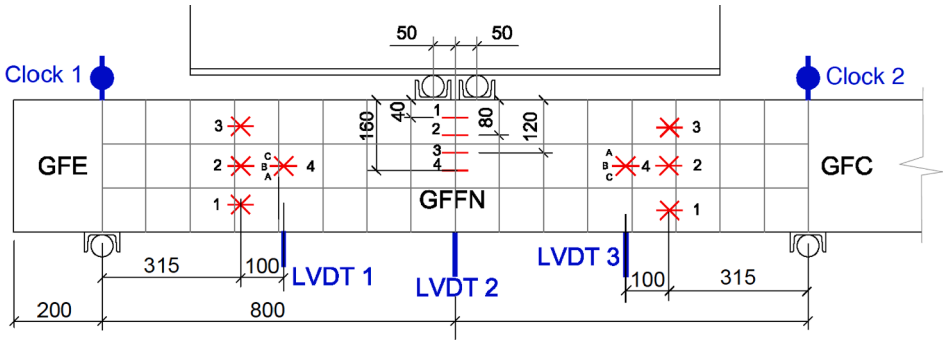

Fig. 2. Instrumentation scheme on the IP beam.

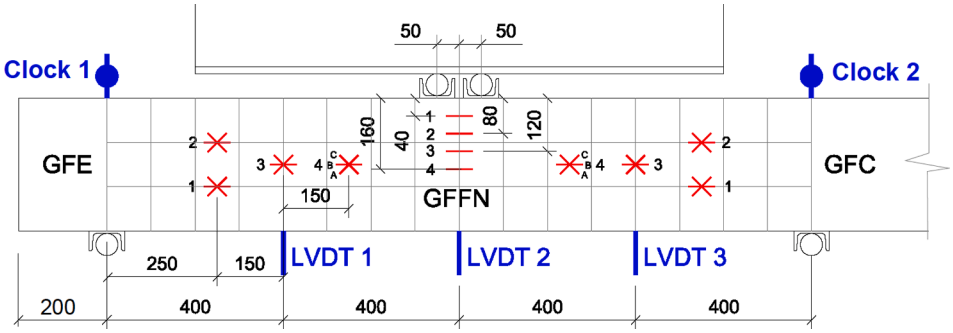

Fig. 3. Instrumentation scheme on the IVP, the ISC and the IVSC beams.

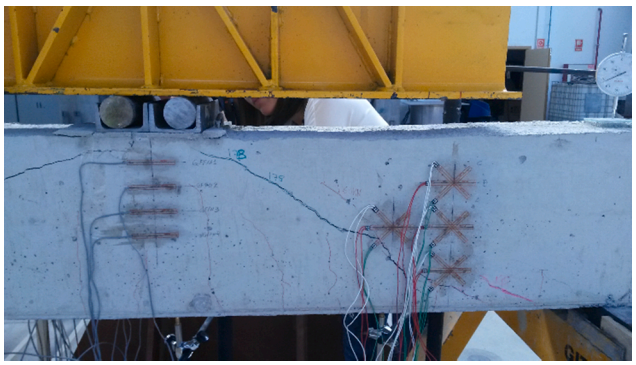

Fig. 5. Right shear span of the IP beam.

Other works have analyzed shear behavior in the case of SRC beams with stirrups when a high transversal steel reinforcement is used. Michelini *et al.* [28] did so by means of different numerical models. Chemrouk and Kong [29] proposed a formula for slender high-strength deep beams. Campione and Cannella [30] proposed an analytical expression for predicting the shear resistance of slender RC beams with stirrups. Demir and Caglar [31] achieved an accurate estimation of the diagonal cracking resistance in deep SRC beams with and without transverse reinforcement by means of a numerical model.

The onset of diagonal cracking during shear loading is usually determined by interrupting the test when the crack becomes visible and annotating the corresponding load value. It may also be done by means of linear crack gauges located at the center of the midspan in a three-point flexural test [16], which are aligned with the principal stress directions. However, these gauge types, due to their large size, make it difficult to place the other experimental instrumentation. It would be interesting to have an alternative experimental methodology, so that the shear cracking load prediction test is not interrupted for visual observation.

The aim of this study is to propose an alternative simple and accurate experimental methodology for the determination of the onset of diagonal cracking in SRC beams under shear loading. This method is based on using conventional extensometric rosette gauges. It was applied to four SRC beams containing Electric Arc Furnace steel slag (EAFS) aggregates and transverse steel reinforcements. The results supported the feasibility of this simple technique when measuring diagonal cracking resistance.

2. Materials

2.1. Concrete

Four types of medium-strength concretes containing EAFS were employed as self-compacting (SC) and pumpable (P) concretes using cement types I and IV: IP, IVP, ISC and IVSC. The concrete components and mix preparation have previously been described by Santamaría *et al.* [9]. The mechanical properties of the concretes are summarized in

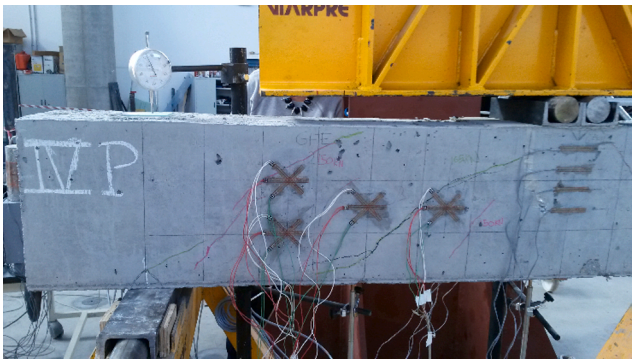

Fig. 7. Left shear span of IVP beam.

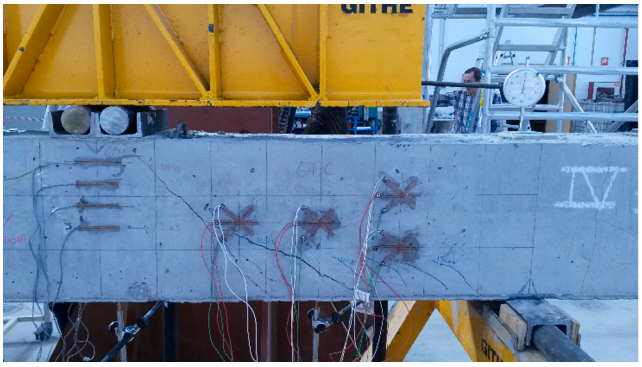

Fig. 8. Right shear span of IVP beam.

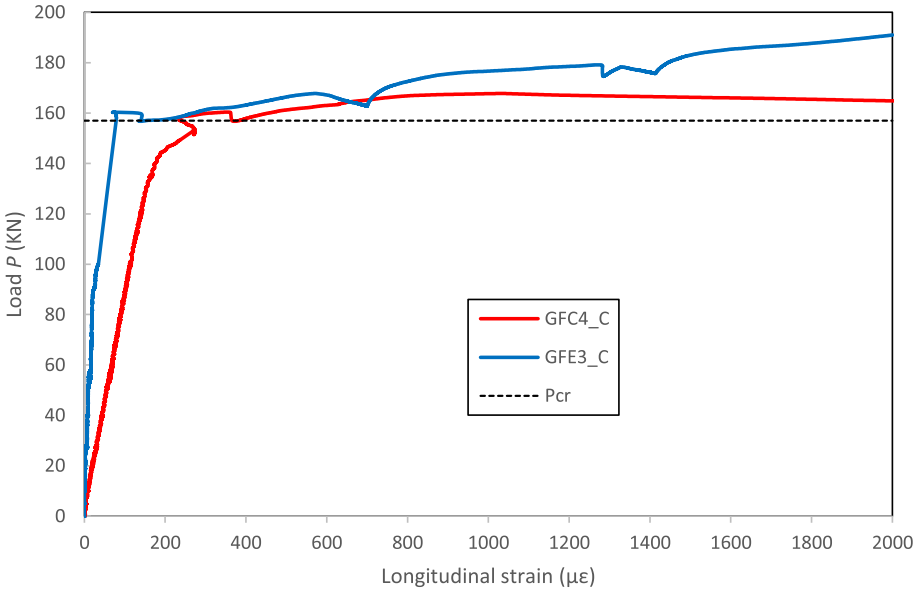

Fig. 6. Load-strain curves of the GFC4_C and GFE3_C gauges on the IP beam.

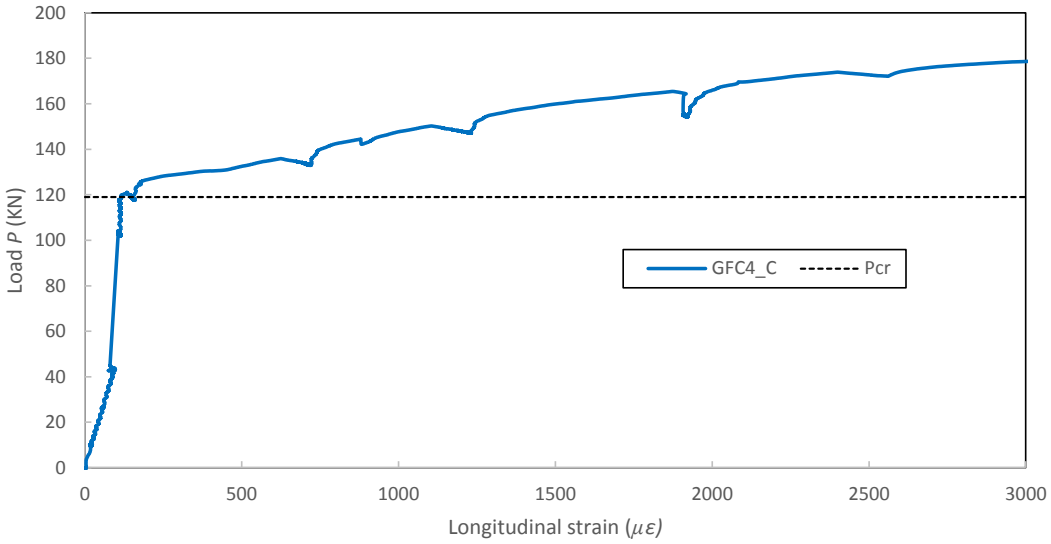

Fig. 9. Load-strain curve of the GFC4_C gauge on the IVP beam.

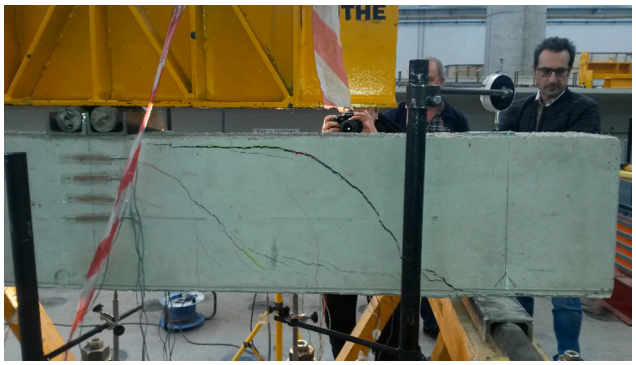

Fig. 10. Dorsal view of the left shear span of the ISC beam.

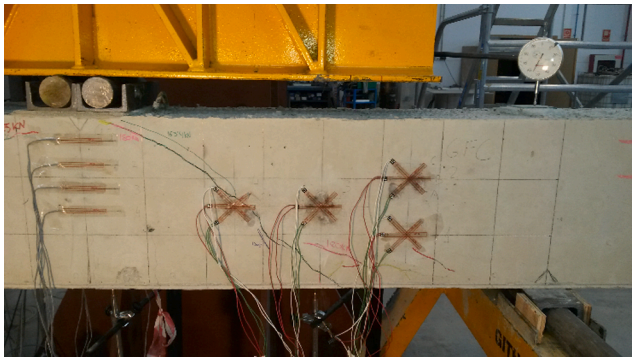

Fig. 11. Right shear span of the ISC beam:

Table 1. The Young's *moduli* and Poisson's ratios were determined according to EN 12390–13 [32]. The compressive strengths were achieved by following EN 12390–3 [33]. In this case, tests were performed at 7–28-90–180-360 days, to assess concrete curing in the moist room. A significant delay in the strength gain of the IVSC concrete was observed when comparing the strength results at 28 days with the corresponding direct tensile strengths at 180 days. The direct tensile strength of the samples, after 180 days in a moist room, measured with the dog bone test (a tensile test used on rocks and high strength concrete) [34] showed a fairly good tensility in the range of 2.5–4.5 MPa.

The experimental results corresponding to the compressive strength after 28 days are given in Table 2. According to EN 12390–3, three specimens were tested at each age, named S1, S2 and S3.

2.2. Steel rebars

Ribbed steel rebars of two diameters (Ø25mm, Ø8mm) were used as longitudinal tensile and compressive reinforcements within the beams. Web reinforcements, consisting of 6-mm diameter vertical closed stirrups were incorporated in the beams. The ribbed steel rebars were manufactured from B 500 S steel, in accordance with the specifications of the UNE 36,068 standard [35]. A rebar yield strength of 525 MPa was considered in the calculations. The yield strength of 525 MPa was considered at a theoretical strain of 4.5 thousandths ($2 + 525/E$(GPa)).

3. Method

A set of four beams was tested. The nominal beam dimension was 200x300x4400 mm. The beams were reinforced with two 25-mm bars in the tension zone ($\rho_l = 0.019$) and two 8-mm bars in the compression zone. A low transversal steel reinforcement was used: 6 mm stirrups spaced at 200 mm. The details on the reinforcement can be seen in Fig. 1.

The diagonal cracking resistance of each beam was tested under three-point flexural loading. In [36], an overview of the development of the experimental techniques employed in shear tests is depicted. However, the use of strain gauges for determining the diagonal cracking load in shear tests has not been found in the literature review. Two pairs of cracks were expected to appear on the lateral sides of the beams corresponding to the left and the right shear spans. Accordingly, the rosette gauges were placed in a first configuration on the IP beam. Then, the direction and the location of the shear cracks observed during the first test were used to relocate them in more suitable positions for the intended purpose in the other tests. The positioning of the rosette gauges for the IP beam is depicted in Fig. 2 and those corresponding to IVP, ISC and IVSC are shown in Fig. 3. The locations of the other instruments relating to the shear test are also shown: GFFN gauges for detecting the neutral axis (both sides, numbered 1 to 4) and LVDTs for measuring the beam deflections. Two additional comparator clocks on the upper face of the beam (clock 1 and clock 2) were positioned on the vertical lines above the supports, for visual readings and to evaluate the settlement of the support system located on the lower face of beam.

The shear span was 750 mm and the effective depth was 258 mm. Therefore, the shear span to effective depth ratio a/d was 2.9 in all cases.

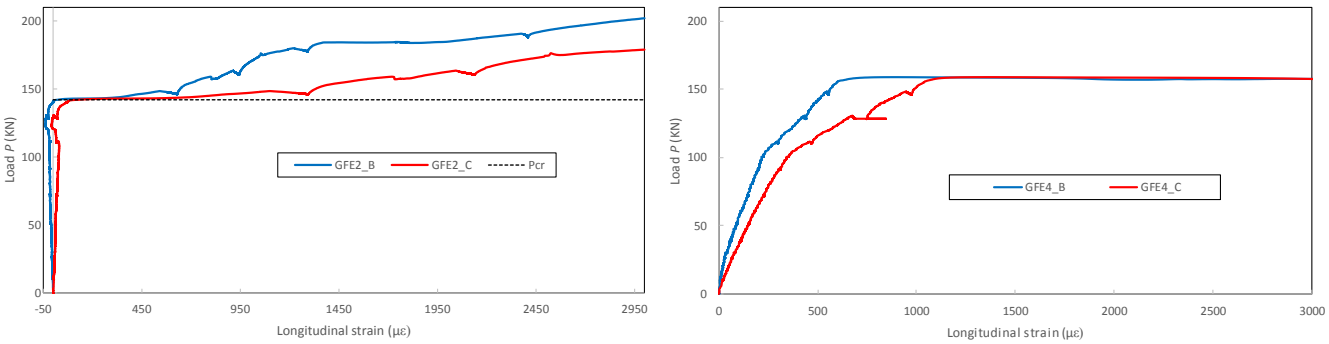

(a) GFE2_B and GFE2_C gauges. (b) GFE4_B and GFE4_C gauges.

Fig. 12. Strain patterns within the ISC beam. (a) GFE2_B and GFE2_C gauges. (b) GFE4_B and GFE4_C gauges.

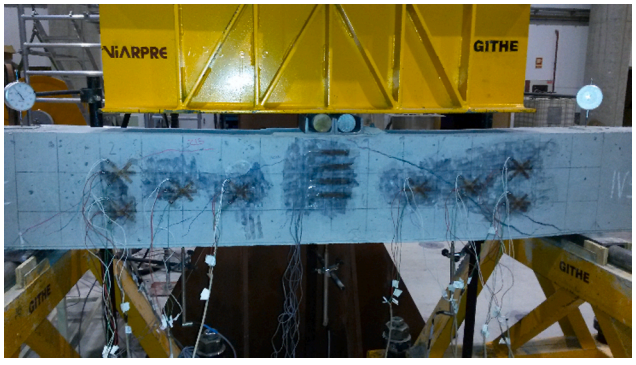

Fig. 13. Front view of the IVSC beam.

In all, 8 rosette strain gauges were used to measure the strain patterns on the lateral surface of the beam. The locations of the onset of diagonal cracking shear resistance were derived from the readings of those gauges (numbered 1 to 4 on both sides of the application load: GFE and GFC).

The two-stage method firstly involved a photographic analysis, in order to detect the gauges through which the diagonal crack propagated. The second stage involved recording the strains that the gauges registered during the test, in order to determine the load value that induced the crack.

4. Results and discussion

In Figs. 4 and 5, the photographs corresponding to the shear failure of the IP beam are shown.

The diagonal cracks passed through the following gauges GFC4_C and GFE3_C.

In Fig. 6, the load–strain curves of the aforementioned gauges are depicted. A plateau may be observed at $P = 157$ KN. Therefore, according to the static problem of the test, the diagonal crack shear resistance was assumed to be $Vcr = P/2 = 78.5$ KN.

In Figs. 7 and 8, the photographs corresponding to the shear failure of the IVP beam are shown.

The cracks propagated through gauges GFE2_C, GFE4_C and GFC4_C. The first diagonal crack appeared in the last gauge, according to the annotations on the beam during the test performance.

In Fig. 9, the load–strain graph of gauge GFC4_C is depicted. The plateau is observed at $P = 119$ KN. The diagonal crack shear resistance

Table 3
Diagonal shear cracking resistance (KN).

	LVDT-s	Present method	Javidmehr	Al-Zoubi	ACI, 2019	Eurocode, 2004
IP	70	78.5	74.79	69.42	62.39	81.23
IVP	52	59.5	61.17	55.87	46.15	66.44
ISC	75	71	74.79	69.42	62.39	81.23
IVSC	70	74	62.54	57.36	47.72	67.93

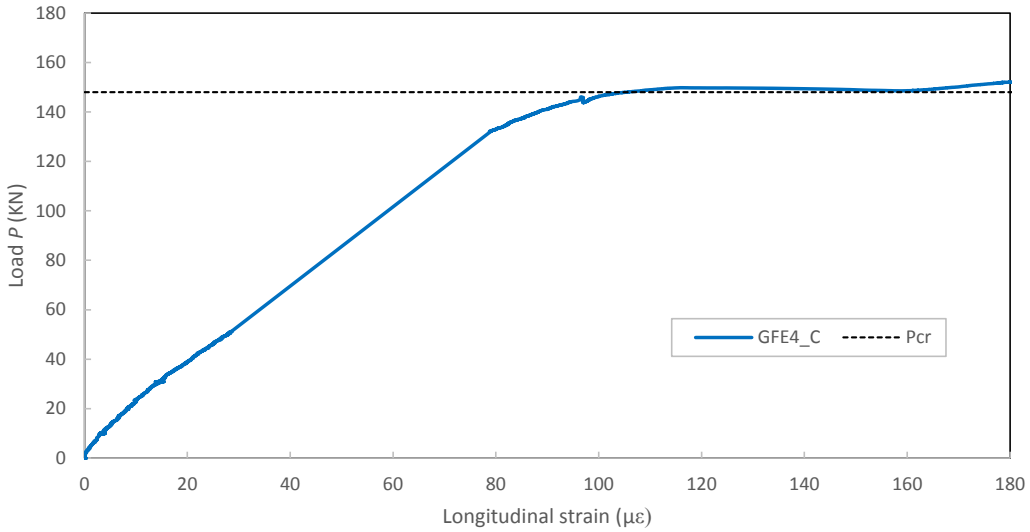

Fig. 14. Load-strain curve of the GFE4_C gauge on the IVSC beam.

was therefore assumed to be $Vcr = P/2 = 59.5$ KN.

In Figs. 10 and 11, the photographs corresponding to the shear failure of the ISC beam are shown.

The first visible diagonal cracks appeared on the lateral side of the left shear span, according to the notes written down on the beam during the test. Thus, the cracks that were assessed had only passed through the strain gauges on the left-hand side: GFE2_B, GFE2_C GFE4_B and GFE4_C.

In Fig. 12, the load–strain curves of the aforementioned gauges are depicted. A plateau was observed at $P = 142$ KN in GFE2_B and GFE2_C gauges. The plateau was located at $P = 150$ KN in relation to the GFE4_B and GFE4_C gauges, which means that the first crack appeared in the former pair of gauges. Therefore, the first value of P was taken into account to determine the diagonal cracking shear resistance: $Vcr = P/2 = 71$ KN.

The photograph in Fig. 13 shows the shear failure of the IVSC beam.

The first diagonal crack appeared to the left of the span, at the GFE4_C gauge, when the load was close to 150 KN, as annotated on the front face of the beam.

In Fig. 14, the load–strain curve of the aforementioned gauge is depicted. A plateau can be observed where the curve flattens out at $P = 148$ KN. Therefore, the diagonal crack shear resistance was equal to: $Vcr = P/2 = 74$ KN.

The values obtained with the proposed method were compared to those using another experimental method based on the Linear Variable Differential Transformer (LVDT) readings at mid span, standard design codes and the approaches proposed by Javidmehr and Al-Zoubi. These authors' formulas were selected because of their greater accuracy than those of other authors and their easy application to the conditions of the present specimens and tests. The results for the diagonal cracking resistance in the SRC beams with a shear-span to depth ratio of 2.9 can be seen in Table 3.

The other experimental method is based on the fact that a peak in the load–displacement curve can be observed at mid span when diagonal cracking occurs [37].

In Table 3, it can be seen that the ACI code yielded more conservative results than Eurocode 2. It is worth underlining that the computations in the case of Eurocode 2 were based on the real properties of the material, and therefore $\gamma_c = 1$ was considered. Moreover, Al-Zoubi's approach appeared more conservative than the one that Javidmehr proposed. The experimental results agree in all the cases under consideration.

The highest discrepancy between the experimental results and those computed with the formulas was noted in the case of the IVSC beam. It was due to the calculations with the analytical expressions based on concrete strength after 28 days. A delay in the strength gain occurred when using cement type IV and the self-compacting concrete. This fact can be seen in Table 3. In the other cases, the agreement between the experimental and analytical results is clear, and that agreement is greater when using the formulas that the aforementioned authors proposed. The experimental results are somewhere between the ACI code and the results for Eurocode 2.

5. Conclusions

An experimental method based on using rosette gauges for predicting diagonal cracking resistance has been proposed in this study.

- Two different gauge schemes have been employed. The second one was more effective at capturing the pair of cracks that delimited the strut. In this case, gauges GFE2, GFE4, GFC2 and GFC4 were decisive when determining the strengths of the different cases.
- The results obtained with the proposed method have been compared to the results of an experimental method based on the LVDT readings, two standard design codes and the approaches proposed by Javidmehr and Al-Zoubi. In general, agreement between all of them was observed except in the case of the IVSC beam, due to the delayed gain of concrete strength.
- ACI yielded more conservative results than Eurocode 2 in all cases. The experimental values were somewhere between both and agreed with the former ones, except in the above-mentioned case.
- The results that were obtained with the formulas of Javidmehr and Al-Zoubi showed better agreement with the experimental results than the results using the two codes.
- Both experimental methods showed good agreement. The proposed method was based on the determination of a plateau in the gauge readings. In the other one, the diagonal cracking shear resistance was determined by locating the peak of the load–displacement curve at mid span.
- The method has yielded results without having to interrupt the test for visual readings and without any subjective visual appraisal of the test specimen.
- The technique could be applied to analyze the diagonal cracking resistance under other conditions and with deep beams.

Declaration of Competing Interest

The authors declare that they have no known competing financial interests or personal relationships that could have appeared to influence the work reported in this paper.

Acknowledgments

The authors wish to express their gratitude to: the Spanish Ministry MICINN, AEI and ERDF [RTI2018-097079-BC31; PID2020-113837RB-I00; 10.13039/501100011033; FPU17/03374]; the Junta de Castilla y León (Regional Government) and ERDF [UIC-231, BU119P17]; Youth Employment Initiative (JCyL) and ESF [UBU05B_1274]; and the University of the Basque Country [PPGA20/26] and **University of Burgos [SUCONS, Y135.GI]** for additional funding. Our thanks also go to the Basque Government research group [IT1314-19] and likewise to CHRYSO and HORMOR for supplying the materials used in this research.

References

[1] Roslan NH, Ismail M, Khalid NHA, Muhammad B. Properties of concrete containing electric arc furnace steel slag and steel sludge. J. Build. Eng. 2020;28:101060. https://doi.org/10.1016/j.jobe.2019.101060.

[2] Lim JS, Cheah CB, Ramli MB. The setting behavior, mechanical properties and drying shrinkage of ternary blended concrete containing granite quarry dust and processed steel slag aggregate. Constr. Build. Mater. 2019;215:447–61. https://doi.org/10.1016/j.conbuildmat.2019.04.162.

[3] Rooholamini H, Sedghi R, Ghobadipour B, Adresi M. Effect of electric arc furnace steel slag on the mechanical and fracture properties of roller-compacted concrete. Constr. Build. Mater. 2019;211:88–98. https://doi.org/10.1016/j.conbuildmat.2019.03.223.

[4] Revilla-Cuesta V, Ortega-López V, Skaf M, Manso JM. Effect of fine recycled concrete aggregate on the mechanical behavior of self-compacting concrete. Constr. Build. Mater. 2020;263:120671. https://doi.org/10.1016/j.conbuildmat.2020.120671.

[5] Revilla-Cuesta V, Skaf M, Chica JA, Fuente-Alonso JA, Ortega-López V. Thermal deformability of recycled self-compacting concrete under cyclical temperature variations. Mater. Lett. 2020;278:128417. https://doi.org/10.1016/j.matlet.2020.128417.

[6] Arribas I, Santamaría A, Ruiz E, Ortega-López V, Manso JM. Electric arc furnace slag and its use in hydraulic concrete. Constr. Build. Mater. 2015;90:68–79. https://doi.org/10.1016/j.conbuildmat.2015.05.003.

[7] Faleschini F, Zanini MA, Toska K. Seismic reliability assessment of code-conforming reinforced concrete buildings made with electric arc furnace slag aggregates. Eng. Struct. 2019;195:324–39. https://doi.org/10.1016/j.engstruct.2019.05.083.

[8] Zanini MA. Structural reliability of bridges realized with reinforced concretes containing electric arc furnace slag aggregates. Eng. Struct. 2019;188:305–19. https://doi.org/10.1016/j.engstruct.2019.02.052.

[9] Santamaría A, Ortega-López V, Skaf M, Chica JA, Manso JM. The study of properties and behavior of self compacting concrete containing Electric Arc Furnace Slag (EAFS) as aggregate. Ain Shams Eng. J. 2020;11(1):231–43. https://doi.org/10.1016/j.asej.2019.10.001.

[10] Ohno, K., Shimozono, S. and Ohtsu, M. (2007), "Cracking mechanisms of diagonal-shear failure monitored and identified by AE-SiGMA Analysis", Proceedings of the 6th International Conference on Fracture Mechanics of Concrete and Concrete Structures, Catania, Italy, June.

[11] Zhang JP. Diagonal cracking and shear strength of reinforced concrete beams. Mag. Concr. Res. 1997;49(178):55–65. https://doi.org/10.1680/macr.1997.49.178.55.
[12] Tanaka Y, Shimomura T, Watanabe M. "Role of diagonal tension crack in size effect of shear strength of deep beams", *Proceedings of FraMCoS-7*. South Korea, May: Jeju; 2010.
[13] Yang KH, Chung HS, Lee ET, Eun HC. Shear characteristics of high-strength concrete deep beams without shear reinforcements. Eng. Struct. 2003;25(10): 1343–52. https://doi.org/10.1016/S0141-0296(03)00110-X.
[14] González-Fonteboa B, Martínez-Abella F. Shear strength of recycled concrete beams. *Constr. Build. Mater.* 2007;21(4):887–93. https://doi.org/10.1016/j.conbuildmat.2005.12.018.
[15] Choi YW, Lee HK, Chu SB, Cheong SH, Jung WY. Shear behavior and performance of deep beams with self-compacting concrete. Int. J. Concr. Struct. Mater. 2012;6 (2):65–78. https://doi.org/10.1007/s40069-012-0007-y.
[16] Demir A, Caglar N, Ozturk H. Parameters affecting diagonal cracking behavior of reinforced concrete deep beams. Eng. Struct. 2019;184:217–31. https://doi.org/10.1016/j.engstruct.2019.01.090.
[17] Słowik M, Nowicki T. The analysis of diagonal crack propagation in concrete beams. Comput. Mater. Sci. 2012;52(1):261–7. https://doi.org/10.1016/j.commatsci.2011.02.012.
[18] Slowik M, Smarzewski P. Study of the scale effect on diagonal crack propagation in concrete beams. Comput. Mater. Sci. 2012;64:216–20. https://doi.org/10.1016/j.commatsci.2012.05.068.
[19] Sato R, Kawakane H. A New Concept for the Early Age Shrinkage Effect on Diagonal Cracking Strength of Reinforced HSC Beams. J. Adv. Concr. Technol. 2008;6(1):45–67. https://doi.org/10.3151/jact.6.45.
[20] Romera JM, Carbajal N, Mujika F. A simple analytical method for determining interlaminar shear stresses in symmetric laminates. Structures 2020;25:683–95. https://doi.org/10.1016/j.istruc.2020.03.053.
[21] ACI 318 (2019), Building Code Requirements for Structural Concrete, American Concrete Institute; Farmington Hills, MI, USA.
[22] Eurocode 2 (2004), Design of Concrete Structures, European Committee for Standardization; Brussels, Belgium.
[23] Thamrin, R., Samad, A.A.A., Chuan, D.Y.E., Hamid, N.A.A. and Ali, I. (2011), "Experimental study on diagonal shear cracks of concrete beams without stirrups longitudinally reinforced with GFRP bars", Proceedings of fib Symposium, Prague, Czech Republic, June.
[24] Wu Xiangguo, Han Sang-Mook. First Diagonal Cracking and Ultimate Shear of I-Shaped Reinforced Girders of Ultra High Performance Fiber Reinforced Concrete without Stirrup. Int. J. Concr. Struct. Mater. 2009;3(1):47–56. https://doi.org/10.4334/IJCSM.2009.3.1.047.
[25] Keskin RSO, Arslan G. Predicting diagonal cracking strength of RC slender beams without stirrups using ANNs. Comput. Concr. 2013;12(5):697–715. https://doi.org/10.12989/cac.2013.12.5.697.
[26] Al-Zoubi MS. Simplified Model for Diagonal Cracking Shear Capacity of Slender RC Beams without Web Reinforcement. Jordan J. Civ. Eng. 2017;11(1):103–16.
[27] Javidmehr S, Oettel V, Empelmann M. Diagonal Cracking of Reinforced Concrete Members Subjected to Shear. Bauingenieur 2018;93:248–54.
[28] Michelini E, Bernardi P, Cerioni R. Failure analysis of RC beams subjected to shear through different numerical approaches. Eng. Fail. Anal. 2017;82:229–42. https://doi.org/10.1016/j.engfailanal.2017.09.006.
[29] Chemrouk M, Kong FK. Diagonal Cracking and Ultimate Shear Strength of Slender High Strength Concrete Deep Beams. Adv. Struct. Eng. 2004;7(3):217–28. https://doi.org/10.1260/136943304323213175.
[30] Campione Giuseppe, Cannella Francesco. Overstrength requirements to avoid brittle shear failure in RC slender beams with stirrups. Eng. Fail. Anal. 2020;118: 104815. https://doi.org/10.1016/j.engfailanal.2020.104815.
[31] Demir A, Caglar N. Numerical determination of crack width for reinforced concrete deep beams. Comput. Concr. 2020;25(3):193–204. https://doi.org/10.12989/cac.2020.25.3.193.
[32] UNE-EN 12390-13, Testing hardened concrete - Part 13: Determination of secant modulus of elasticity in compression, AENOR; Madrid, Spain.
[33] UNE-EN 12390-3, Testing hardened concrete - Part 3: Compressive strength of test specimens, AENOR; Madrid, Spain.
[34] Zhou Z, Qiao P. Direct tension test for characterization of tensile behavior of Ultra-High Performance Concrete. J. Test. Eval. 2020;48(4):2730–49. https://doi.org/10.1520/JTE20170644.
[35] UNE 36068 (2011), Barras corrugadas de acero soldable para uso estructural en armaduras de hormigón armado, AENOR; Madrid, Spain.
[36] Schacht G, Bolle G, Steffen M. Measuring in shear tests - Technical Development and actual possibilities. Beton- Stahlbetonbau 2013;108(12):875–86. https://doi.org/10.1002/best.201300050.
[37] Ignjatović IS, Marinković SB, Tošić N. Shear behaviour of recycled aggregate concrete beams with and without shear reinforcement. Eng. Struct. 2017;141: 386–401. https://doi.org/10.1016/j.engstruct.2017.03.026.